Effects of bradykinin on TGF-β1-induced epithelial-mesenchymal transition in ARPE-19 cells

QINGQUAN WEI[1], QINGYU LIU[1], CHENGDA REN[1], JUNLING LIU[1], WENTING CAI[1], MEIJIANG ZHU[1], HUIZI JIN[1], MENGMEI HE[2] and JING YU[1]

[1]Department of Ophthalmology, Shanghai Tenth People's Hospital Affiliated with Tongji University, Shanghai 200072; [2]Department of Ophthalmology, The First Affiliated Hospital of Xi'an Jiaotong University, Xi'an, Shanxi 710061, P.R. China

Received December 30, 2016; Accepted December 15, 2017

DOI: 10.3892/mmr.2018.8556

Abstract. The aim of the present study was to investigate the effects of bradykinin (BK) on an epithelial-mesenchymal transition (EMT) model in retinal pigment epithelium (RPE) cells through exposure to transforming growth factor-β1 (TGF-β1). The aim was to improve the effect of BK on proliferative vitreoretinopathy (PVR) progression, and to find a novel method of clinical prevention and treatment for PVR. The morphology of ARPE-19 cells was observed using an inverted phase-contrast microscope. A Cell Counting Kit-8 was used to assess the effects of TGF-β1 on the proliferation of ARPE-19 cells. Western blotting and immunofluorescence were used to detect the expression levels of the epithelial marker E-cadherin, mesenchymal markers α-smooth muscle actin (SMA) and vimentin, and phosphorylated (p) mothers against decapentaplegic homolog (Smad)3 and Smad7 of the TGF/Smad signaling pathway. Wound healing tests and Transwell assays were performed to detect cell migration ability. Reverse transcription-quantitative polymerase chain reaction (RT-qPCR) analysis was performed to detect the expression levels of pSmad3 and Smad7 in the TGF/Smad signaling pathway. The results revealed that the addition of 10 ng/ml TGF-β1 resulted in the expression of factors associated with EMT in ARPE-19 cells. BK decreased the expression levels of the mesenchymal markers α-SMA and vimentin, and increased the expression of the epithelial marker E-cadherin. BK decreased cell migration in TGF-β1-induced EMT. These effects were reversed by HOE-140, a specific BK 2 receptor antagonist. BK significantly downregulated the expression of pSmad3 and upregulated the expression of Smad7 in TGF-β1-treated ARPE-19 cells, and the protective alterations produced by BK were inhibited by HOE-140. In conclusion, 10 ng/ml TGF-β1 resulted in EMT in ARPE-19 cells and BK served a negative role in TGF-β1-induced EMT. BK had effects in TGF-β1-induced EMT by upregulating the expression of Smad7 and downregulating the expression of pSmad3 in TGF-β/Smad signaling pathway, indicating that BK may be a novel and effective therapy for PVR.

Correspondence to: Dr Mengmei He, Department of Ophthalmology, The First Affiliated Hospital of Xi'an Jiaotong University, 277 Yanta Road, Xi'an, Shanxi 710061, P.R. China
E-mail: hemengmeiwqq@163.com

Dr Jing Yu, Department of Ophthalmology, Shanghai Tenth People's Hospital Affiliated with Tongji University, 301 Middle Yanchang Road, Shanghai 200072, P.R. China
E-mail: dryujing@aliyun.com

Key words: bradykinin, proliferative vitreoretinopathy, transforming growth factor-β1, epithelial-mesenchymal transition, retinal pigment epithelium

Introduction

Proliferative vitreoretinopathy (PVR) is a clinical syndrome that occurs following rhegmatogenous retinal detachment and is caused by breaks in the retina, including retinal tears, retinal holes or surgical repair. The basic pathophysiological process is damage to the blood-retinal barrier. A variety of cells participate in PVR, including retinal pigment epithelium (RPE) cells, glial cells, fibroblasts and inflammatory cells (1). RPE cells are the primary component of the cell proliferation membrane and are the dominant cell in the pathogenesis of PVR (2). The main pathophysiological mechanism of PVR is considered to be the conversion of RPE cells into mesenchymal cells via epithelial-mesenchymal transition (EMT) (3). A number of studies have observed the prevention of PVR by inhibiting EMT (4,5). However, the molecular mechanism underlying transforming growth factor (TGF)-β1-induced EMT is poorly understood.

EMT may be induced and regulated by various factors, including TGF-β, thrombin, platelet-derived growth factor and bone morphogenetic proteins (6). TGF-β-induced EMT has been investigated in the majority of epithelial cell types (7). Expression of the TGF family is upregulated in the vitreous or epiretinal proliferative membranes in patients with PVR (8,9). In addition, TGF-β expression levels are positively associated with the severity of PVR in vitreous or PVR experimental models (10). Blocking the TGF-β signaling pathway may inhibit the conversion of RPE cells via EMT *in vivo* and *in vitro* (11,12). Therefore, TGF-β serves an important role in the pathogenesis of PVR. TGF-β1 resulted in EMT of RPEs

and the development of PVR, which has become a classical model of EMT (13,14).

Studies have reported that chronic inflammation has a role in the pathogenesis of PVR (15) and is an important pathological factor for promoting the development of proliferative retinopathy. The complement and blood coagulation cascades are the most important Kyoto Encyclopedia of Genes and Genomes (KEGG) pathways in the pathological process of PVR (16). The cascade consists of the kinin-kallikrein system (KKS), the blood coagulation system and the complement system. As the intermediate process connecting the complement pathway and thrombin, the KKS serves a key role in regulation. The KKS is primarily composed of kallikrein, kininogen, kinin, bradykinin 1 receptor (B1R), bradykinin 2 receptor (B2R) and kininase. Kinin includes bradykinin (BK) and kallidin (KD), and KD may be converted into BK under the action of enzymes. Therefore, BK, as the final effector molecule, is the primary kinin under physiological conditions. The expression of BK is significantly increased in experimental animal models with severe PVR (17). Therefore, it was hypothesized in the present study that BK may regulate KKS, the blood coagulation system and the complement system, and ultimately act via KEGG pathways to induce PVR. To elucidate the underlying mechanisms behind PVR and enhance its treatment in a clinical setting, the role of BK in its pathophysiology requires further investigation.

Materials and methods

Cell culture. Human retinal pigment epithelial cells (ARPE-19) were obtained from Cell Biosciences Pty, Ltd. (Heidelberg, Australia). ARPE-19 cells were cultured in Dulbecco's modified Eagle's medium (DMEM)/H (Gibco; Thermo Fisher Scientific, Inc., Waltham, MA, USA) supplemented with 10% fetal bovine serum (FBS; Gibco; Thermo Fisher Scientific, Inc.). Cells were incubated at 37˚C in a humidified incubator containing 5% CO_2. The cell culture medium was changed every 3-4 days. At 50-70% confluence, the cells were growth-arrested in serum-free medium for 12 h at 37˚C prior to the addition of 10 nM BK for 0.5 h. Subsequently, 10 ng/ml TGF-β1 (PeproTech, Inc., Rocky Hill, NJ, USA) was added for 48 h at 37˚C. The TGF-β1 concentration and incubation time were determined from dose response experiments (0 to 12.5 ng/ml) and time course experiments (24 and 48 h) to induce EMT and provide the optimal balance between cytotoxicity and cell viability (Fig. 1A). B2R activity was blocked by pre-incubating the cells for 1 h at 37˚C with 100 uM of the B2R antagonist, HOE-140 (Sigma-Aldrich; Merck KGaA, Darmstadt, Germany).

Cell Counting Kit-8 (CCK-8) assay. ARPE-19 cells were seeded into 96-well plates at $5x10^3$ cells/well and cultured in DMEM. At 50% confluence, the medium was replaced with FBS-free medium, and culture was continued for 12 h. TGF-β1 (0, 0.1, 0.5, 2.5, 10 and 12.5 ng/ml) was added to the medium as aforementioned. Then ARPE-19 cells were incubated for 24 and 48 h respectively at 37˚C in a humidified incubator containing 5% CO_2. CCK-8 reagents (Nanjing AnboRuila Biotechnology Co., Ltd., Nanjing, China) were added to each well and incubated at 37˚C for 4 h. The absorbance was measured at a wavelength of 450 nm using an ELISA plate reader (BioTek China, Beijing, China).

Cell morphology. ARPE-19 cells were seeded into 6-well plates at $5x10^5$ cells/well containing DMEM with 10% FBS. After reaching 70% confluence, the medium was replaced with FBS-free medium, and culture was continued for 12 h at 37˚C. A total of 100 nM BK, 10 ng/ml TGF-β1, 100 nM BK plus 10 ng/ml TGF-β1, 10 ng/ml TGF-β1 plus 10 uM HOE140, 100 nM BK plus 10 ng/ml TGF-β1 plus 10 uM HOE140, or DMEM/H vehicle, was added to the medium. The cells were growth-arrested in serum-free medium for 12 h at 37˚C prior to the addition of BK for 0.5 h. Subsequently, TGF-β1 was added for 48 h at 37˚C. B2R activity was blocked by pre-incubating the cells for 1 h at 37˚C with of the B2R antagonist, HOE-140. The morphological alterations were observed with an inverted phase-contrast microscope (Shanxi AntaiGroup Co., Ltd., Shanxi, China, magnification, x100). A total of five fields were analyzed and experiments were repeated three times in duplicate.

Western blot analysis. ARPE-19 cells were homogenized using lysis buffer containing 50 mM Tris (pH 7.4), 150 mM NaCl, 1% Triton X-100, 1% sodium deoxycholate, 0.1% SDS, 5 mM sodium orthovanadate, 5 mM EDTA, 1 mM phenylmethanesulfonyl fluoride and 1 mM NaF. Total protein was quantified by bicinchoninic acid assay (Beyotime Institute of Biotechnology, Haimen, China). A total of 25 μg protein was analyzed for EMT-associated protein expression, including the epithelial marker E-cadherin, the mesenchymal markers α-smooth muscle actin (SMA) and vimentin, and phosphorylated (p) mothers against decapentaplegic homolog (Smad)3 and Smad7. Protein samples were subjected to SDS-PAGE (6-12% polyacrylamide gels) and transferred onto a polyvinylidene diflouride membrane (EMD Millipore, Billerica, MA, USA). Membranes were blocked with 5% non-fat milk for 1 h at 37˚C and probed with antibodies overnight at 4˚C. The antibodies and dilution ratios were as follows: Anti-E-cadherin (1:500; cat. no. GTX100443, GeneTex International Corporation, Hsinchu, Taiwan), mouse anti-α-SMA (1:500; cat. no. BS70000, Bioworld Technology, Inc., St. Louis Park, MN, USA), vimentin (cat. no. BS1491, 1:500; Bioworld Technology, Inc.), anti-pSmad3 (1:500; cat. no. BS4173, Bioworld Technology, Inc.), anti-Smad7 (1:500; cat. no. BS60366, Bioworld Technology, Inc.) and anti-GAPDH (1:500; cat. no. G9545, Sigma-Aldrich; Merck KGaA). Following washing with 0.1% TBS-Tween 20 containing 5% skim milk at room temperature, membranes were incubated with horseradish peroxidase-conjugated sheep anti-mouse secondary antibodies (1:2,000; cat. no. A5906, Sigma-Aldrich; Merck KGaA) or peroxidase-conjugated goat anti-rabbit secondary antibodies (1:2,000; cat. no. A6154, Sigma-Aldrich; Merck KGaA) for 1 h at room temperature. Image Quant LAS 4000 (GE Healthcare, Chicago, IL, USA) with ImageJ software (version 1.38e, National Institutes of Health, Bethesda, MD, USA) were used to quantify band intensities.

Cell immunofluorescence analysis. ARPE-19 cells were seeded into 24-well plates at $4x10^4$ cells/well containing DMEM with 10% FBS. After reaching 70% confluence, the

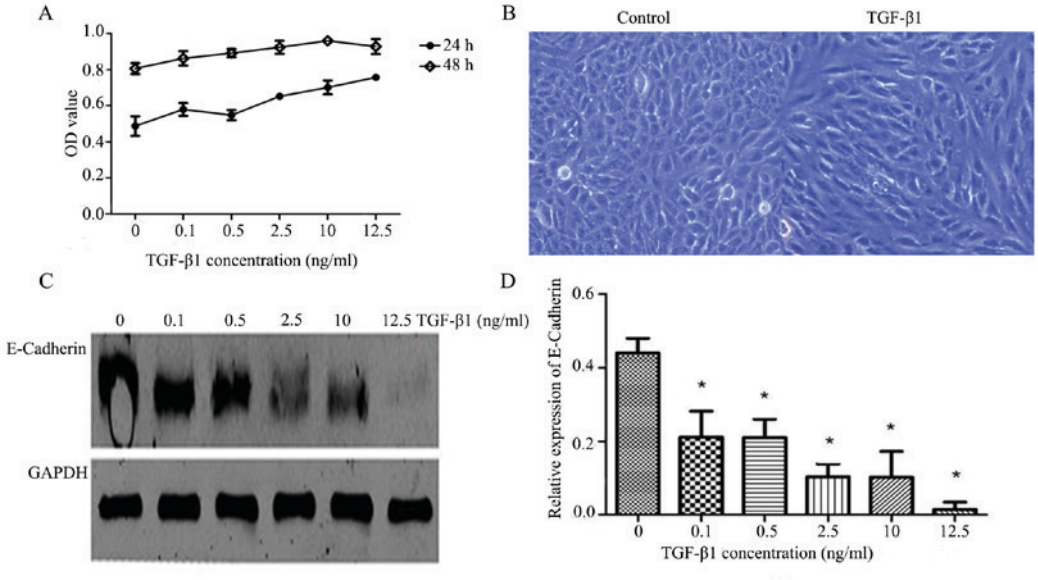

Figure 1. Treatment with 10 ng/ml TGF-β1 for 48 h results in epithelial-mesenchymal transition-associated features. (A) Different concentrations of TGF-β1 affected the proliferation of ARPE-19 cells. (B) Morphological alterations were detected between the control group and the TGF-β1 group using an inverted phase-contrast microscope (magnification, x100). The optimal concentration of TGF-β1 was 10 ng/ml and the optimal incubation time was 48 h. (C) Western blot analysis was used to detect the expression levels of E-cadherin with different concentrations of TGF-β1, and (D) the results were quantified. All experiments were performed in triplicate. *P<0.05 vs. control. TGF-β1, transforming growth factor-β1; OD, optical density.

medium was replaced with FBS-free medium, and culture was continued for 12 h at 37˚C. Following treatment with 100 nM BK, 10 ng/ml TGF-β1, 100 nM BK plus 10 ng/ml TGF-β1, 10 ng/ml TGF-β1 plus 10 uM HOE140, or 100 nM BK plus 10 ng/ml TGF-β1 plus 10 uM HOE140, or DMEM/H vehicle, was added to the medium. The cells were growth-arrested in serum-free medium for 12 h at 37˚C prior to the addition of BK for 0.5 h. Subsequently, TGF-β1 was added for 48 h at 37˚C. B2R activity was blocked by pre-incubating the cells for 1 h at 37˚C with of the B2R antagonist, HOE-140. Then cells of different groups were washed three times with PBS and fixed with 4% paraformaldehyde for 20 min at room temperature. Following three washings with PBS, cells were blocked with 10% bovine serum albumin (1:2,000; cat. no. B2064, Sigma-Aldrich; Merck KGaA) for 30 min at 37˚C and incubated overnight at 4˚C with the primary antibodies described above. The dilutions were as follows: Rabbit anti-E-cadherin (1:100), mouse anti-a-SMA (1:100), vimentin (1:100), anti-p Smad3 (1:100) and anti-Smad7 (1:100). Cells were stained with FITC-labeled goat anti-rabbit immunoglobulin G (1:500; cat. no. F0382, Sigma-Aldrich; Merck KGaA) for 2 h at 37˚C andDAPI (1:5,000; cat. no. D9542, Sigma-Aldrich; Merck KGaA) for 5 min at 37˚C to visualize the nuclei. Images were captured using a confocal microscope (Zeiss GmbH, Jena, Germany, magnification, x200).

Wound healing test. ARPE-19 cells were seeded in six-well plates at a density of $5x10^5$ cells/well and cultured with DMEM/H containing 10% FBS. At 70-80% confluence, the cells were serum-starved for 12 h at 37˚C. A total of 100 nM BK, 10 ng/ml TGF-β1, 100 nM BK plus 10 ng/ml TGF-β1, 10 ng/ml TGF-β1 plus 10 uM HOE140, 100 nM BK plus 10 ng/ml TGF-β1 plus 10 uM HOE140, or DMEM/H vehicle, was added to the medium. The cells were growth-arrested in serum-free medium for 12 h at 37˚C prior to the addition of BK for 0.5 h. Subsequently, TGF-β1 was added for 48 h at 37˚C. B2R activity was blocked by pre-incubating the cells for 1 h at 37˚C with of the B2R antagonist, HOE-140. A sterile 200 μl pipette tip was used to create a wound in the monolayer by scraping. The cells were washed with PBS and cultured in FBS-free medium for 24 h at 37˚C in a humidified incubator containing 5% CO_2. Micrographs were captured with an inverted phase contrast microscope (magnification, x50). Experiments were repeated three times in duplicate.

Transwell migration assay. ARPE-19 cells were seeded in six-well plates at a density of $5x10^5$ cells/well and cultured with DMEM/H containing 10% FBS. At 50-70% confluence, the cells were starved for 12 h at 37˚C. Cells were treated as aforementioned. A total of $1x10^6$ cells were added to the top chamber of 24-well Transwell plates (8 μm pore size; Corning Incorporated, Corning, NY, USA) in 200 μl medium. The bottom chambers were filled with 500 μl medium with 5% FBS. Following 18 h of incubation at 37˚C in the 5% CO_2 atmosphere, and the chambers were then washed with PBS. Cells that did not invade through the membrane were removed, while the invading cells on the lower surface of the membrane, were fixed with 4% paraformaldehyde for 15 min at room temperature and then stained with 0.1% crystal violet for 20 min at room temperature. The number of migratory cells in each chamber was quantified by counting five fields under a light microscope (OLYMPUS CKX41; Olympus Corporation, Tokyo, Japan, magnification, x50). Another counting method was used, where cells were bleached with 33% acetic acid for 15 min at room temperature following staining with 0.1% crystal violet, prior to adding CCK-8 reagent (Nanjing AnboRuila Biotechnology Co., Ltd.) to the eluent. The optical density value was measured at a wavelength of 570 nm using

Table I. Primers used for reverse transcription-quantitative polymerase chain reaction amplification.

Gene	Forward 5'→3'	Reverse 5'→3'
pSmad3	TGGACGCAGGTTCTCCAAAC	CCGGCTCGCAGTAGGTAAC
Smad7	GGACAGCTCAATTCGGACAAC	GTACACCCACACACCATCCAC
GAPDH	AGAAGGCTGGGGCTCATTTG	AGGGGCCATCCACAGTCTTC

pSmad, phosphorylated mothers against decapentaplegic homolog.

an ELISA plate reader (BioTek China). All experiments were repeated at least three times.

Reverse transcription-quantitative polymerase chain reaction (RT-qPCR). Total RNA of cells was extracted using TRIzol reagent, according to the manufacturer's protocol (Invitrogen; Thermo Fisher Scientific, Inc.). The concentration of RNA was measured with a Nanodrop 2000 spectrophotometer (Thermo Fisher Scientific, Inc., Wilmington, DE, USA), and cDNA was synthesized from 1 μg total RNA using a PrimeScript™ RT-PCR kit (cat. no. RR037A; Takara Biotechnology Co., Ltd., Dalian, China). Specific primers (Bioworld Technology, Inc.) were used to detect the expression of EMT-associated genes, using GAPDH as an internal control. miRNA quantification was performed using the 7500 Fast Real-time PCR system (Applied Biosystems; Thermo Fisher Scientific, Inc.) using a SYBR®PrimeScript™ RT-qPCR kit (cat. no. RR081A; Takara Bio, Inc.). The 20 μl reaction system contained the following: 10 μl SYBR Premix Ex Taq (2X), 0.4 μl ROX Dye II, 6 μl dH_2O, 0.8 μl PCR forward primer, 0.8 μl PCR reverse primer and 2 μl cDNA. qPCR thermal cycling was performed as follows: One cycle at 95˚C for 30 sec, followed by 40 cycles of 95˚C for 5 sec and 60˚C for 34 sec, and one cycle of 95˚C for 15 sec, 60˚C for 30 sec and 95˚C for 15 sec for fluorescence signal acquisition. The relative quantity of each gene was measured using the $2^{-\Delta\Delta Cq}$ method (18). All RT-qPCR experiments were performed in triplicate. Primer sequences are listed in Table I.

Statistical analysis. Independent sample t-test was used for two-group comparisons. One-way analysis of variance followed by a Student-Newman-Keuls test, was used for multiple sample analysis. P<0.05 was considered to indicate a statistically significant difference. The data were analyzed with SPSS version 19.0 software (IBM Corp., Armonk, NY, USA). The data were expressed as the mean ± standard deviation.

Results

Treatment with 10 ng/ml TGF-β1 induced EMT in ARPE-19 cells. To assess the optimal concentration and time of treatment with TGF-β1 that resulted in the success of the experimental EMT model in ARPE-19 cells, a CCK-8 assay was used to investigate cell proliferation. TGF-β1-treated groups had elevated optical density values compared with the control group (Fig. 1A). ARPE-19 cell proliferation was more obvious following 48 h TGF-β1 treatment compared with 24 h, and cell proliferation was most marked when the concentration of TGF-β1 was 10 ng/ml at 48 h (Table II and Fig. 1A). An inverted phase-contrast microscope was used to observe the cell morphology. ARPE-19 cell morphology was altered compared with the control group at 10 ng/ml TGF-β1 and 48 h. Cell morphology gradually changed from the typical cobblestone-like to the long spindle-shaped mesenchymal-like cells (Fig. 1B). In addition, the expression levels of E-cadherin were detected by western blot analysis. When ARPE-19 cells were treated with different concentrations of TGF-β1 for 48 h, E-cadherin expression was reduced compared with the control group (P<0.05; Fig. 1C and D). E-cadherin expression in ARPE-19 cells was negatively associated with TGF-β1 concentration (Fig. 1C and D). Therefore, the EMT experimental model was successfully established when ARPE-19 cells were treated with TGF-β1 (10 ng/ml) for 48 h. This time point was chosen to examine the function of BK in the following experiments.

Table II. Different concentrations of TGF-β1 affect the proliferation of ARPE-19 cells.

Concentration of TGF-β1 (ng/ml)	Optical density value	
	24 h	48 h
0	0.49±0.05	0.81±0.02
0.1	0.58±0.04[a]	0.86±0.02[a]
0.5	0.55±0.03[a]	0.89±0.01[a]
2.5	0.65±0.01[a]	0.92±0.01[a]
10	0.70±0.04[a]	0.96±0.02[a]
12.5	0.76±0.01[a]	0.93±0.01[a]

[a]P<0.05 vs. TGF-β1 at 0 ng/ml. TGF-β1, transforming growth factor-β1.

BK inhibits TGF-β1-induced EMT in ARPE-19 cells, and the B2R inhibitor attenuates the role of BK. To determine whether BK serves an important role in TGF-β1-induced EMT, the alterations in cell morphology were observed and the expression levels of E-cadherin, α-SMA and vimentin in each group were determined. Fig. 2A demonstrated that BK+TGF-β1 group may prevent TGF-β1-induced EMT; the number of spindle-shaped mesenchymal cells decreased, whereas BK+TGF-β1+HOE-140 weakened the role of BK and the mesenchyme transformation of the cells increased significantly. Western blot analysis revealed that BK+TGF-β1 group increased E-cadherin protein expression levels, and decreased the expression levels of α-SMA and vimentin

compared with TGF-β1-treated cells (P<0.05). The B2R inhibitor HOE-140 in BK+TGF-β1+HOE-140 group blocked BK, weakening its effect compared with BK+TGF-β1 group (P<0.05, Fig. 2B). The immunofluorescence results revealed that BK in BK+TGF-β1 group significantly attenuated the downregulation of E-cadherin, and the upregulation of α-SMA and vimentin compared with TGF-β1-treated cells, whereas B2R antagonism in BK+TGF-β1+HOE-140 group reversed this effect compared with BK+TGF-β1group (Fig. 2C). In addition, BK in BK+TGF-β1 group inhibited the ARPE-19 cell migration enhanced by TGF-β1. With HOE-140 in BK+TGF-β1+HOE-140 group, cell migration ability was enhanced compared with BK+TGF-β1 group (Table III; Fig. 2D-F). These results suggested that BK may inhibit TGF-β1-induced EMT in ARPE-19 cells.

BK inhibits TGF-β1-induced EMT in ARPE-19 cells via the TGF/Smad signaling pathway. To determine whether BK inhibits TGF-β1-induced EMT in ARPE-19 cells via the TGF/Smad signaling pathway, pSmad3 and Smad7 expression levels were measured. As determined by western blot analysis (Fig. 3A), BK+TGF-β1 group decreased pSmad3 protein expression levels and increased Smad7 protein expression levels compared with TGF-β1-treated cells. The expression levels of pSmad3 and Smad7 were reversed by treatment with the B2R antagonist HOE-140 in BK+TGF-β1+HOE-140 group compared with BK+TGF-β1 group. These changes in pSmad3 and Smad7 mRNA expression were verified by q-PCR (Fig. 3B). Immunofluorescence revealed that BK+TGF-β1 group markedly downregulated the expression of pSmad3 and upregulated the expression of Smad7 compared with TGF-β1-treated ARPE-19 cells, molecular events that were antagonized by HOE140 (Fig. 3C). These results demonstrated that BK had effects on TGF-β1-induced EMT by upregulating the expression of Smad7 and downregulating the expression of pSmad3 in the TGF-β/Smad signaling pathway.

Table III. The effect of TGF-β1 on migration of ARPE-19 cells.

A, Migration distance of ARPE-19 cells

Group	Migration distance, μm (mean ± standard deviation)
DMEM (control)	3.60±0.62
BK	3.53±0.50
TGF-β1	3.98±0.36
TGF-β1+BK	3.55±0.47
TGF-β1+HOE-140	3.86±0.22
TGF-β1+BK+HOE-140	3.77±0.32

B, Optical density value of cell migration using the indirect enumeration method

Group	Optical density value (mean ± standard deviation)
DMEM (control)	0.431±0.059
BK	0.430±0.054
TGF-β1	1.272±0.059[a]
TGF-β1+BK	0.562±0.018[b]
TGF-β1+HOE-140	1.208±0.038
TGF-β1+BK+HOE-140	0.666±0.048[c]

[a]P<0.001 vs. DMEM group, [b]P<0.001 vs. TGF-β1 group and [c]P<0.05 vs. TGF-β1+BK group. TGF-β1, transforming growth factor-β1; BK, bradykinin; DMEM, Dulbecco's modified Eagle's medium.

Discussion

PVR is generally considered to be an afibrotic process driven by EMT in RPE cells, causing traction of the retina and leading to surgical failure (19). EMT widely exists in renal interstitial fibrosis (20) and liver fibrosis (21). EMT has a vital role in the recurrence of liver cancer (22), in addition to the occurrence and metastasis of lung cancer (23). TGF may be divided into three subtypes in mammals: TGF-β1, TGF-β2 and TGF-β3. TGF-β1 is a multi-effective growth factor, and it is the primary cytokine that mediates EMT in tumor cells (24). TGF-β1-induced EMT of RPE cells has been acknowledged as a classic model to study the underlying mechanisms of EMT (13,14). However, the optimal concentration and time of treatment with TGF-β1 may differ (25-27).

In the present study, different concentrations of TGF were used to treat ARPE-19 cells for 24 and 48 h, and it was observed that 10 ng/ml TGF-β1 resulted in EMT of ARPE-19 cells. The alteration in cell morphology was more marked when the TGF-β treatment time was 48 h, compared with 24 h. This result was consistent with the results of Yang *et al* (27). The integrity of cell-cell contacts is an important regulator of TGF-β1-induced epithelial-to-myofibroblast transition (28). E-cadherin is a principal component of adhesive connections between cells. This suggests that E-cadherin may be involved in TGF-β1-induced EMT. E-cadherin is highly expressed in normal ARPE-19 cells (29). When E-cadherin transcription is suppressed, it may affect adhesion between epithelial cells and eventually result in EMT. Therefore, decreased E-cadherin is an indicator of EMT in epithelial cells (30). In the present study, western blot analysis was used to detect the expression levels of E-cadherin in cells. The results revealed that the E-cadherin expression levels were increased in normal ARPE-19 cells. With increased TGF-β1 concentration, the expression level of E-cadherin was gradually reduced. This demonstrated that the TGF-β1-induced EMT model was successfully established *in vitro*.

At present, there is no safe and effective clinical drug used as a conventional treatment for PVR (31). Vitreous cavity injection of polylactic acid, daunorubicin or 5-fluorouracil in rabbit eyes following vitrectomy may effectively prevent the formation of PVR membranes (32). In addition, anti-inflammatory drugs, including triamcinolone acetonide, and intravitreal injections as an adjunct to vitrectomy and silicone oil tamponade, appear to be effective and safe in treating PVR (grade C or D) (33). Anti-inflammatory therapy in PVR may be a potential research direction.

The complement and blood coagulation cascades are the most important KEGG pathways in the PVR pathological process, and the KKS is the intermediate process connecting

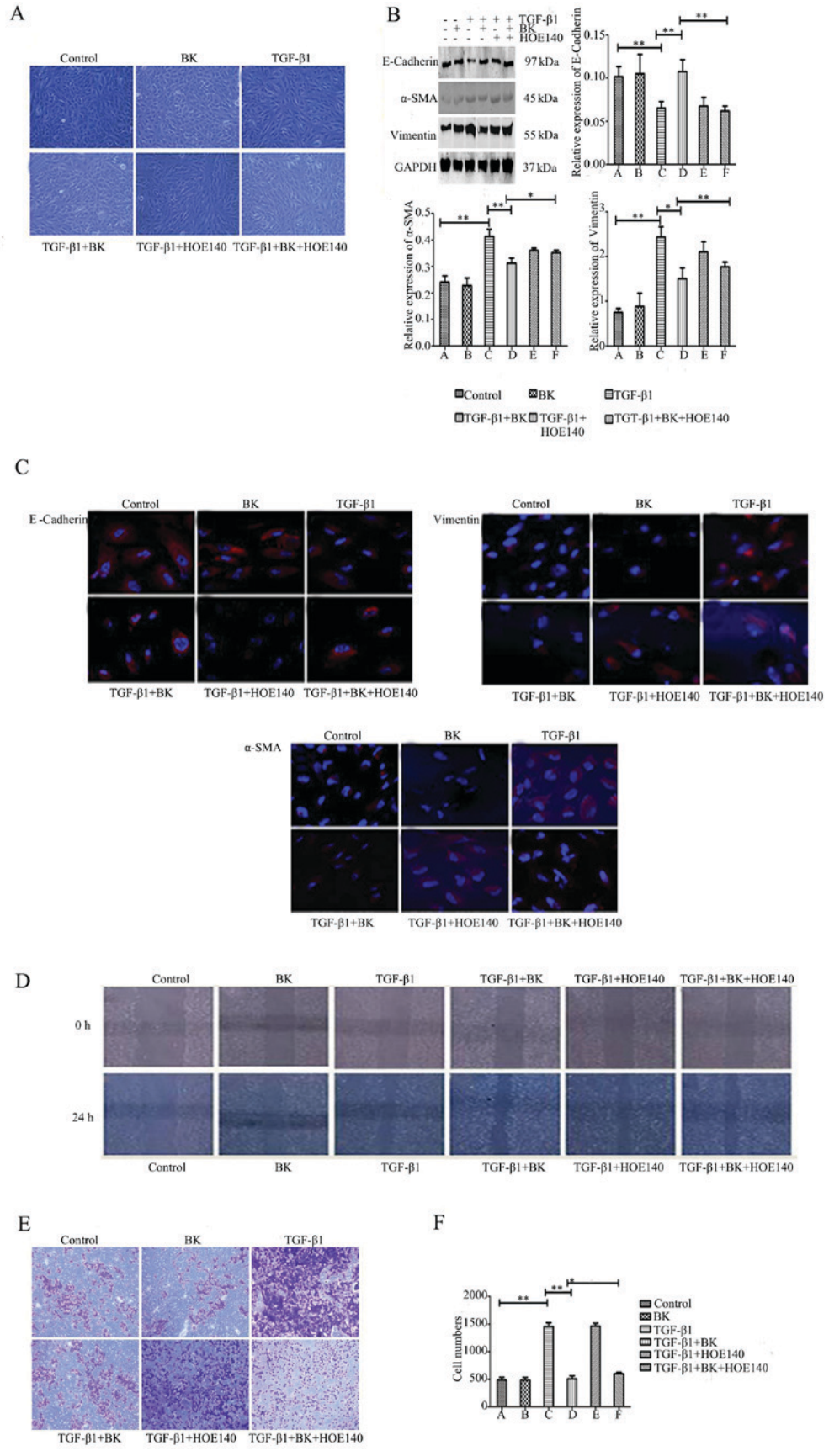

Figure 2. BK inhibits TGF-β1-induced epithelial-mesenchymal transitionin ARPE-19 cells, and a B2R inhibitor attenuates the role of BK. ARPE-19 cells were treated with BK, TGF-β1, BK plus TGF-β1, TGF-β1 plus HOE140, BK plus TGF-β1 plus HOE140, and Dulbecco's modified Eagle's medium for 48 h prior todetection. (A) Morphological alterations were detected using an inverted phase-contrast microscope (magnification, x100). (B) Western blot analysis detected the expression levels of E-cadherin, α-SMA and vimentin in each group. (C) The protein expression of E-cadherin, α-SMA and vimentin was identified by immunofluorescence staining (magnification, x200). (D) A wound healing assay tested the cell migration of a scratched edge. (E) Cells that had migrated through the Transwell chamber filter over 18 h were stained with crystal violet, and imaged at x50 magnification. (F) The number of migrated ARPE-19 cells in each group. **P<0.001 and *P<0.05. TGF-β1, transforming growth factor-β1; BK, bradykinin; α-SMA, α-smooth muscle actin.

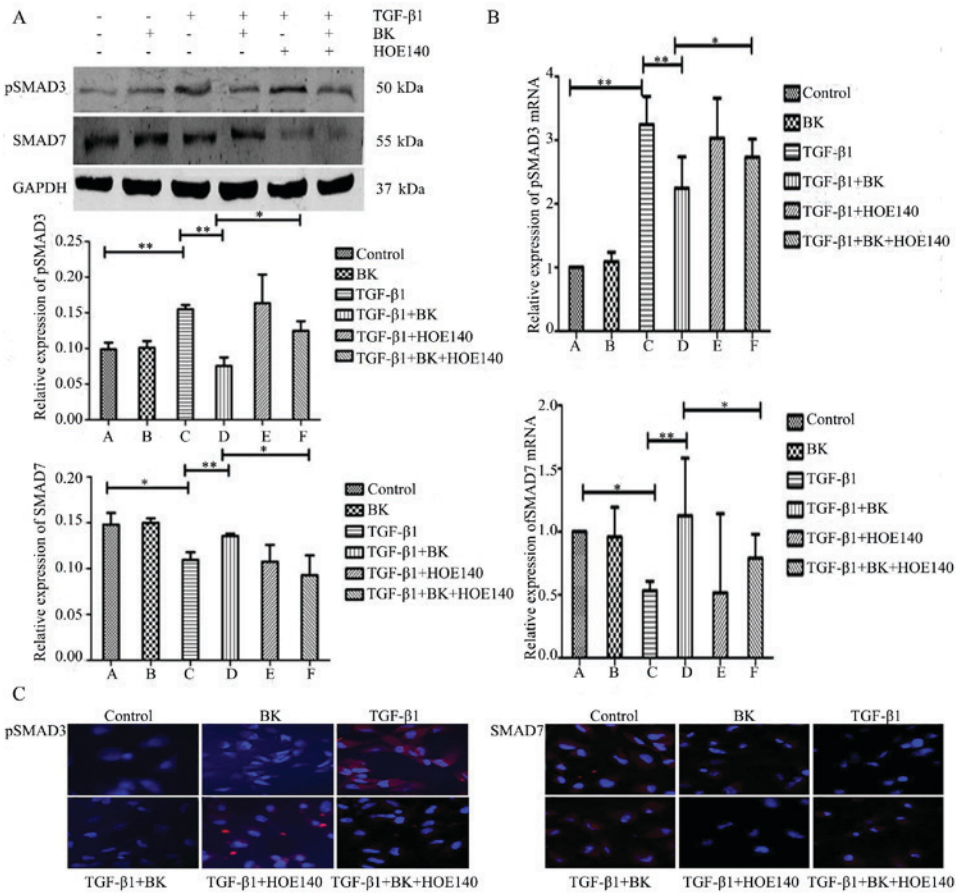

Figure 3. BK inhibits TGF-β1-induced epithelial-mesenchymal transition via the TGF/Smad signaling pathway. ARPE-19 cells were treated with BK, TGF-β1, BK plus TGF-β1, TGF-β1 plus HOE140, BK plus TGF-β1 plus HOE140 and Dulbecco's modified Eagle's medium for 48 h before detection. (A) Protein expression of pSmad3 and Smad7 was identified by western blot analysis. (B) Reverse transcription-quantitative polymerase chain reaction analysis and (C) immunofluorescence staining (magnification, x200). **P<0.001 and *P<0.05. TGF-β1, transforming growth factor-β1; BK, bradykinin; pSmad, phosphorylated mothers against decapentaplegic homolog.

the complement pathways and the blood coagulation pathway (16). KKS serves an important role in inflammation (34). In the KKS system, activated kallikrein acts on kininogen. Plasma kininases convert high molecular weight kininogen to BK and kallidin, whereas tissue kininases convert low molecular weight kininogen to kallidin, which may be converted into BK under the action of enzymes (35). The BK amino acid sequence is Arg-Pro-Pro-Gly-Phe-Ser-Pro-Phe-Arg, and it has a series of complex physiological effects with kinin receptors in tissues and organs (36). The BK receptor is divided into B1R and B2R. B2R serves a primary role in biological reactions. It is expressed in a variety of cell types, including myocardial cells, pain sensitive neurons, endothelial cells and smooth muscle cells (37). BK protects renal function via B2R receptors in renal fibrosis, and this effect may be reversed by a B2R receptor antagonist (38). To examine whether BK has a similar effect in PVR disease, the present study used BK to stimulate PVR in an *in vitro* cell model to observe the influence of BK on PVR models. In the present study, it was demonstrated that BK has effects on the protein expression levels in TGF-β1-induced EMT and reverses EMT. It increased epithelial cell marker protein levels and decreased interstitial cell marker protein levels. Vitreous aspirates from patients with PVR stimulate retinal pigment epithelial cell migration (39). Research has recently focused on investigating RPE cell migration (40,41). To further determine whether BK influences TGF-β1-induced EMT migration, a wound healing assay and the Transwell migration method was used. It was revealed that BK inhibited ARPE-19 cell migration. With HOE-140, the cell migration ability was enhanced.

The TGF-β/Smad pathway is a major component of the process of the phenotype alteration from epithelial cells to mesenchymal cells (42,43). TGF-β combines with the TGF-β type II receptor and forms a closely linked complex with TGF-β type I receptor, which leads to Smad2 and Smad3 activation. The activated Smad2 and Smad3 bind with Smad4 for target gene recognition and transcriptional regulation (44-46). Although the function of pSmad2 and pSmad3 is certain in this process, a previous study demonstrated that Smad3 is the essential mediator of TGF-β signaling and directly activates genes encoding regulators of transcription and signal transducers (47). Smad7 negatively regulates Smad2/3, and its overexpression inhibits EMT in RPE cells (48). Smad3 is required for the de-differentiation of the retinal pigment epithelium following retinal detachment. Blocking the Smad3 pathway may inhibit the occurrence of EMT (14). Upregulation of the BK-B2R pathway modulates the TGF-β/Smad signaling cascade to reduce renal fibrosis (38). However, the function of BK in RPE cells is

unknown. In the present study, it was determined that BK reduced pSmad3 expression levels and increased Smad7 expression levels. The protective alterations were reversed by HOE-140. However, the present results were only verified *in vitro*; whether the same conclusion is observed *in vivo* requires further investigation.

In conclusion, the results of the present study suggested that BK contributes to the progression of TGF-β1-mediated EMT in ARPE-19 cells via the TGF/Smad signaling pathway. These findings may promote a future clinical therapeutic strategy for the prevention or treatment of PVR.

Acknowledgements

The present study was financially supported by the National Natural Science Foundation of China (grant no. 81470648). The authors would like to thank the Central Laboratory of Shanghai Tenth People's Hospital Affiliated with Tongji University for the experimental facilities and equipment.

References

1. Pennock S, Haddock LJ, Eliott D, Mukai S and Kazlauskas A: Is neutralizing vitreal growth factors aviable strategy to prevent proliferative vitreoretinopathy? Prog Retin Eye Res 40: 16-34, 2014.
2. Umazume K, Tsukahara R, Liu L, Fernandez de Castro JP, McDonald K, Kaplan HJ and Tamiya S: Role of retinal pigment epithelial cell β-catenin signaling in experimental proliferative vitreoretinopathy. Am J Pathol 184: 1419-1428, 2014.
3. Tosi GM, Marigliani D, Romeo N and Toti P: Disease pathways in proliferative vitreoretinopathy: An ongoing challenge. J Cell Physiol 229: 1577-1583, 2014.
4. Li H, Wang H, Wang F, Gu Q and Xu X: Snail involves in the transforming growth factor β1-mediated epithelial-mesenchymal transition of retinal pigment epithelial cells. PLoS One 6: e23322, 2011.
5. Bartel DP: MicroRNAs: Target recognition and regulatory functions. Cell 136: 215-233, 2009.
6. Yang S, Li H, Li M and Wang F: Mechanisms of epithelial-mesenchymal transition in proliferative vitreoretinopathy. Discov Med 20: 207-217, 2015.
7. Zhang J, Tian XJ, Zhang H, Teng Y, Li R, Bai F, Elankumaran S and Xing J: TGF-β-induced epithelial-to-mesenchymal transition proceeds through stepwise activation of multiple feedback loops. Sci Signal 7: ra91, 2014.
8. Bochaton-Piallat ML, Kapetanios AD, Donati G, Redard M, Gabbiani G and Pournaras CJ: TGF-beta1, TGF-beta receptor II and ED-A fibronectin expression in myofibroblast of vitreoretinopathy. Invest Ophthalmol Vis Sci 41: 2336-2342, 2000.
9. Asaria RH, Kon CH, Bunce C, Sethi CS, Limb GA, Khaw PT, Aylward GW and Charteris DG: Silicone oil concentrates fibrogenic growth factors in the retro-oil fluid. Br J Ophthalmol 88: 1439-1442, 2004.
10. Hoerster R, Muether PS, Vierkotten S, Hermann MM, Kirchhof B and Fauser S: Upregulation of TGF-ß1 in experimental proliferative vitreoretinopathy is accompanied by epithelial to mesenchymal transition. Graefes Arch Clin Exp Ophthalmol 252: 11-16, 2014.
11. Liang CM, Tai MC, Chang YH, Chen YH, Chen CL, Lu DW and Chen JT: Glucosamine inhibits epithelial-to-mesenchymal transition and migration of retinal pigment epithelium cells in culture and morphologic changes in a mouse model of proliferative vitreoretinopathy. Acta Ophthalmol 89: e505-e514, 2011.
12. Nassar K, Grisanti S, Tura A, Lüke J, Lüke M, Soliman M and Grisanti S: A TGF-β receptor 1 inhibitor for prevention of proliferative vitreoretinopathy. Exp Eye Res 123: 72-86, 2014.
13. Dvashi Z, Goldberg M, Adir O, Shapira M and Pollack A: TGF-β1 induced transdifferentiation of RPE cells is mediated by TAK1. PLoS One 10: e0122229, 2015.
14. Saika S, Kono-Saika S, Tanaka T, Yamanaka O, Ohnishi Y, Sato M, Muragaki Y, Ooshima A, Yoo J, Flanders KC and Roberts AB: Smad3 is required for dedifferentiation of retinal pigment epithelium following retinal detachment in mice. Lab Invest 84: 1245-1258, 2004.
15. Garweg JG, Tappeiner C and Halberstadt M: Pathophysiology of proliferative vitreoretinopathy in retinal detachment. Surv Ophthalmol 58: 321-329, 2013.
16. Yu J, Peng R, Chen H, Cui C and Ba J: Elucidation of the pathogenic mechanism of rhegmatogenous retinal detachment with proliferative vitreoretinopathy by proteomic analysis. Invest Ophthalmol Vis Sci 53: 8146-8153, 2012.
17. Zhao HM, Yu J, Sheng MJ and Wang KS: Experimental study of kallikrein-kinin system participating in proliferative vitreoretinopathy procedure. Chin J Exp Ophthalmol 29: 591-595, 2011 (In Chinese).
18. Livak KJ and Schmittgen TD: Analysis of relative gene expression data using real-time quantitative PCR and the 2(-Delta DeltaC(T)) method. Methods 25: 402-408, 2001.
19. Saika S, Yamanaka O, Okada Y, Tanaka S, Miyamoto T, Sumioka T, Kitano A, Shirai K and Ikeda K: TGF-beta in fibroproliferative diseases in the eye. Front Biosci (Schol Ed) 1: 376-390, 2009.
20. Bai Y, Lu H, Lin C, Xu Y, Hu D, Liang Y, Hong W and Chen B: Sonic hedgehog-mediated epithelial-mesenchymal transition in renal tubulointerstitial fibrosis. Int J Mol Med 37: 1317-1327, 2016.
21. Zhao YL, Zhu RT and Sun YL: Epithelial-mesenchymal transition in liver fibrosis. Biomed Rep 4: 269-274, 2016.
22. Wu TJ, Chang SS, Li CW, Hsu YH, Chen TC, Lee WC, Yeh CT and Hung MC: Severe hepatitis promotes hepatocellular carcinoma recurrence via NF-κB pathway-mediated epithelial-mesenchymal transition after resection. Clin Cancer Res 22: 1800-1812, 2016.
23. Hong SK, Park JR, Kwon OS, Kim KT, Bae GY and Cha HJ: Induction of integrin β3 by sustained ERK activity promotes the invasiveness of TGFβ-induced mesenchymal tumor cells. Cancer Lett 376: 339-346, 2016.
24. Massagué J: TGF-beta in cancer. Cell 134: 215-230, 2008.
25. Han L, Zhang HW, Zhou WP, Chen GM and Guo KJ: The effects of genistein on transforming growth factor-β1-induced invasion and metastasis in human pancreatic cancer cell line Panc-1 in vitro. Chin Med J (Engl) 125: 2032-2040, 2012.
26. Koeck S, Amann A, Huber JM, Gamerith G, Hilbe W and Zwierzina H: The impact of metformin and salinomycin on transforming growth factor β-induced epithelial-to-mesenchymal transition in non-small cell lung cancer cell lines. Oncol Lett 11: 2946-2952, 2016.
27. Yang S, Yao H, Li M, Li H and Wang F: Long non-coding RNA MALAT1 mediates transforming growth factor beta1-induced epithelial-mesenchymal transition of retinal pigment epithelial cells. PLoS One 11: e0152687, 2016.
28. Masszi A, Fan L, Rosivall L, McCulloch CA, Rotstein OD, Mucsi I and Kapus A: Integrity of cell-cell contacts is a critical regulator of TGF-beta 1-induced epithelial-to-myofibroblast transition: Role for beta-catenin. Am J Pathol 165: 1955-1967, 2004.
29. Palma-Nicolás JP and López-Colomé AM: Thrombin induces slug-mediated E-cadherin transcriptional repression and the parallel up-regulation of N-cadherin by a transcription-independent mechanism in RPE cells. J Cell Physiol 228: 581-589, 2013.
30. Cano A, Pérez-Moreno MA, Rodrigo I, Locascio A, Blanco MJ, del Barrio MG, Portillo F and Nieto MA: The transcription factor snail controls epithelial-mesenchymal transitions by repressing E-cadherin expression. Nat Cell Biol 2: 76-83, 2000.
31. Priglinger CS and Priglinger S: Pharmacological approach to treatment of proliferative vitreoretinopathy. Ophthalmology 110: 948-959, 2013 (In German).
32. Mandava N, Blackburn P, Paul DB, Wilson MW, Read SB, Alspaugh E, Tritz R, Barber JR, Robbins JM and Kruse CA: Ribozyme to proliferating cell nuclear antigen to treat proliferative vitreoretinopathy. Invest Ophthalmol Vis Sci 43: 3338-3348, 2002.
33. Chen W, Chen H, Hou P, Fok A, Hu Y and Lam DS: Midterm results of low-dose intravitreal triamcinolone as adjunctive treatment for proliferative vitreoretinopathy. Retina 31: 1137-1142, 2011.

34. Yarovaya GA and Neshkova EA: Kallikrein-Kinin system. Long history and present. (To 90th Anniversary of Discovery of the System). Bioorg Khim 41: 275-291, 2015 (In Russian).
35. Wang T, Tang Y and Lou JS: Advances in research on kallikrein-kinin system in cardiovascular system. Chin J Pharmacol Toxicol 17: 466-470, 2003.
36. Yu J, Peng R, Chen H, Cui C, Ba J and Wang F: Kininogen 1 and insulin-like growth factor binding protein 6: Candidate serum biomarkers of proliferative vitreoretinopathy. Clin Exp Optom 97: 72-79, 2014.
37. Leeb-Lundberg LM, Marceau F, Müller-Esterl W, Pettibone DJ and Zuraw BL: International union of pharmacology. XLV. Classification of the kinin receptor family: From molecular mechanisms to pathophysiological consequences. Pharmacol Rev 57: 27-77, 2005.
38. Cárdenas A, Campos J, Ehrenfeld P, Mezzano S, Ruiz-Ortega M, Figueroa CD and Ardiles L: Up-regulation of the kinin B2 receptor pathway modulates the TGF-β/Smad signaling cascade to reduce renal fibrosis induced by albumin. Peptides 73: 7-19, 2015.
39. Campochiaro PA, Jerdan JA, Glaser BM, Cardin A and Michels RG: Vitreous aspirates from patients with proliferative vitreoretinopathy stimulate retinal pigment epithelial cell migratio. Arch Ophthalmol 103: 1403-1405, 1985.
40. He S, Kuma SR, Zhou P, Krasnoperov V, Ryan SJ, Gill PS and Hinton DR: Soluble EphB4 inhibition of PDGF-induced RPE migration in vitro. Invest Ophthalmol Vis Sci 51: 543-552, 2010.
41. Chan CM, Huang JH, Chiang HS, Wu WB, Lin HH, Hong JY and Hung CF: Effects of (-)-epigallocatechin gallate on RPE cell migration and adhesion. Mol Vis 16: 586-595, 2010.
42. Lamouille S, Xu J and Derynck R: Molecular mechanisms of epithelial-mesenchymal transition. Nat Rev Mol Cell Biol 15: 178-196, 2014.
43. Saitoh M and Miyazawa K: Transcriptional and post-transcriptional regulation in TGF-β-mediated epithelial-mesenchymal transition. J Biochem 151: 563-571, 2012.
44. Choi K, Lee K, Ryu SW, Im M, Kook KH and Choi C: Pirfenidone inhibits transforming growth factor-β1-induced fibrogenesis by blocking nuclear translocation of Smads in human retinal pigmentepithelial cell line ARPE-19. Mol Vis 18: 1010-1020, 2012.
45. Feng XH and Derynck R: Specificity and versatility in tgf-beta signaling through Smads. Annu Rev Cell Dev Biol 21: 659-693, 2005.
46. Massagué J: TGF-β signalling in context. Nat Rev Mol Cell Biol 13: 616-630, 2012.
47. Yang YC, Piek E, Zavadil J, Liang D, Xie D, Heyer J, Pavlidis P, Kucherlapati R, Roberts AB and Böttinger EP: Hierarchical model of gene regulation by transforming growth factor beta. Proc Natl Acad Sci USA 100: 10269-10274, 2003.
48. Saika S, Yamanaka O, Nishikawa-Ishida I, Kitano A, Flanders KC, Okada Y, Ohnishi Y, Nakajima Y and Ikeda K: Effect of Smad7 gene overexpression on transforming growth factor beta-induced retinal pigment fibrosis in a proliferative vitreoretinopathy mouse model. Arch Ophthalmol 125: 647-654, 2007.